ISPRS Annals of the Photogrammetry, Remote Sensing and Spatial Information Sciences, Volume X-G-2025
ISPRS Geospatial Week 2025 "Photogrammetry & Remote Sensing for a Better Tomorrow…", 6–11 April 2025, Dubai, UAE

Crowdsourced Indoor Positioning: Integrating 5G NR and WiFi Technologies

Peng Ye[1], Liang Chen[1*]

[1]State Key Laboratory of Information Engineering in Surveying, Mapping and Remote Sensing (LIESMARS), Wuhan University, Hubei Province, China - (ye_peng, l.chen)@whu.edu.cn

Keywords: Crowdsourcing, indoor position, path cluster, inflection point, WiFi, 5G NR.

Abstract

Indoor positioning technology is a key area of research in location-based services. Crowdsourced WiFi and mobile communication signal fingerprinting are critical for achieving large-scale indoor positioning for consumers. However, existing crowdsourced positioning solutions are not suitable for typical environments like shopping malls due to the need for additional equipment, and their learning methods often have low computational efficiency and generalization ability in complex environments. This paper proposes a system that introduces clustering concepts to repair remaining trajectories using representative trajectories. WiFi SSID and 5G NR SSB data collected along trajectories are used as features for clustering analysis. Reliable starting points are obtained through GNSS accuracy metrics to correct trajectories, and a Bi-LSTM model is utilized to extract trajectory inflection points. Unprocessed trajectories of the same category are corrected based on inflection point features, thereby constructing a WiFi-5G fingerprint database. In addition to providing positioning services, the proposed system iteratively infers the locations of shops, allowing for the construction of a semantic map. The experimental site is the first floor of a large shopping mall, with a dataset comprising 185 user-collected trajectories totaling 2 hours in duration. The trajectory clustering accuracy exceeds 80%, with an average localization error of 5.73 meters for static test points, and an average error of 4.38 meters for the semantic map. Compared to existing crowdsourced solutions, the proposed method shows significant improvements in feasibility, accuracy, and efficiency.

1. Introduction

Location is a crucial attribute of IoT information, and sensed data without location is meaningless. With the gradual improvement of Global Navigation Satellite Systems (GNSS) and the continuous innovation of corresponding positioning technologies, acquiring high-precision outdoor location information is no longer a challenge (Groves, 2015). However, obtaining high-precision location data in indoor environments, where GNSS signals cannot reach, has become a significant area of interest.

Currently, commonly used indoor positioning signal sources include WiFi, geomagnetic signals, acoustic signals and mobile communication signals. (Ruizhi and Liang, 2017) Based on these signals, researchers propose positioning methods that are either geometric or fingerprint-based (Jang and Kim, 2018). Geometric methods can be further divided into ranging and angle-based approaches (Ruan et al., 2022), which mainly include Time of Arrival, Time Difference of Arrival and Angle of Departure. However, due to the complex multipath effects that occur during signal propagation in intricate environments, geometric positioning methods face significant limitations. Consequently, fingerprint-based positioning methods have gained more favor among researchers.

Fingerprint positioning, a relatively mature method, typically involves two phases (Jang and Kim, 2018): the offline phase, which is the database creation stage, and the online phase, which is the positioning stage. During the offline phase, wireless signal data is collected at various reference points (RPs) within a designated area. The collected signal data is then associated with corresponding geographical locations to create a detailed fingerprint map. In the online phase, user devices collect real-time wireless signal features as they move. These features are compared with the fingerprint database to identify the best-matching reference point, thus determining the user's current location. The signal characteristics of different sources vary during the positioning process. For WiFi (Bellavista-Parent et al., 2021), the focus is on the differences in signal strength from multiple Access Points (APs). In the case of 5G NR signals (Yang et al., 2024), the focus is on the similarity in the shapes of multi-beam signals. For geomagnetic signals (Sun et al., 2021), the focus is on changes in signal strength over continuous time periods. Fingerprint positioning effectively transforms the localization problem into a classification challenge, leading to the increasing incorporation of learning algorithms in this field. (Ruan et al., 2023) utilizes unsupervised deep autoencoder networks to reconstruct 5G Channel State Information (CSI) features. Generally, fingerprint-based methods demonstrate relatively high accuracy; however, the costs associated with on-site data collection and periodic updates limit their broader application.

Interpolation and crowdsourcing technologies are increasingly employed for the rapid updating of fingerprint databases. In terms of interpolation techniques, (Lan et al., 2022) proposed a fingerprint enhancement framework based on super-resolution. Regarding crowdsourcing, (Wang et al., 2023) achieved crowdsourced geomagnetic database construction through a learning-based trajectory recovery algorithm and keyframe association technology, resulting in an average localization error of 2.53 meters. Due to significant limitations in data consistency and applicability (Liu et al., 2023), interpolation methods are gradually being overshadowed by crowdsourcing as the primary means of quickly updating fingerprint databases.

In the field of consumer-grade wide-area indoor positioning, areas with dense coverage of WiFi and mobile communication signals (Hu et al., 2022) predominantly favor the construction of WiFi and 5G signal maps based on crowdsourced data. (Junoh and Pyun, 2023) employed Bluetooth Low Energy beacons for trajectory calibration and introduced a generative adversarial network-based approach to enhance the fingerprint database. (Zhao et al., 2020) integrated crowdsourced data into a graph-based representation and applied multidimensional scaling algorithms to calculate users' walking points. However, these methods still face challenges in demanding application scenarios: 1) They often require additional infrastructure, such as Bluetooth Low Energy beacons, leading to increased costs as the area expands and resulting in lower availability; 2) In complex environments like large shopping malls, the computational efficiency of learning methods is low, and their generalizability is limited.

To achieve consumer-grade wide-area indoor positioning, further exploration of relevant technologies is necessary. This paper presents a new crowdsourcing-based solution for constructing WiFi and 5G signal maps and positioning. Compared to existing solutions, the main contributions of this paper are summarized as follows.

1) When handling crowdsourced data to obtain an accurate fingerprint database, we introduce the concept of clustering, which uses high-quality trajectories within a cluster for overall trajectory correction, compared with the traditional independent analysis of a single path. In terms of clustering, based on the spatial openness of shopping malls and the abundance of WiFi devices, we use WiFi SSID count features instead of trajectory shape features for path clustering. Additionally, we refine the clustering results with the help of 5G NR signals.

2) Compared with the traditional method of trajectory correction based on known access point (AP) locations, we iteratively derive more reliable information about interest point locations and construct semantic maps using corrected trajectory data in conjunction with the free propagation model.

The remainder of the article is structured as follows. The system flow of the crowdsource data processing method proposed in this paper is described in Section 2. Section 3 presents the experimental setup, experimental results and related discussions. Finally, Section 4 summarizes the article.

2. Methodology of Fingerprinting Based on Crowdsourced Data

2.1 System Overview

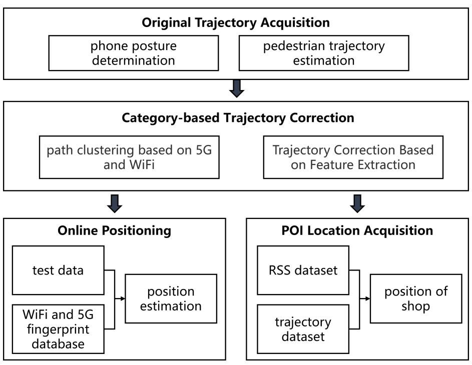

Figure 1. System overview

Fig. 1 summarizes the specific processing flow of the system proposed in this paper. The system processes crowdsourced data with landmark location information to construct a WiFi + 5G fingerprint database in scenarios where map information is unavailable and inertial navigation data is uncalibrated. First, a trained posture classification model is used to determine the mobile carrying mode, facilitating trajectory estimation for users who consistently hold their phones. Next, for users switching layers on the same escalator, clustering analysis is performed using the WiFi SSID data collected prior to the switch as features, with further corrections made using 5G data. A Bi-LSTM model is employed to extract trajectory inflection points, while GNSS accuracy indicators provide reliable starting points for trajectory correction. Unprocessed trajectories of the same category are corrected based on inflection point features. Subsequently, corresponding WiFi data is obtained using the timestamps of the calibrated trajectories, and store location information is iteratively inferred based on a free-space propagation model to construct a semantic map. Finally, the location information of all calibrated trajectories is matched with positioning signal data to build the fingerprint database, enabling high-precision and highly usable indoor positioning.

2.2 Trajectory Inference by Pedestrian Dead Reckoning

In this study, we utilized a self-sampled dataset for model training, focusing on classifying mobile phone carrying modes. We performed trajectory estimation for users who maintained a handheld mode throughout their walking phase. As shown in Fig. 2, we categorized mobile phone carrying modes into handheld mode, left-hand calling mode, right-hand calling mode, left-hand swinging mode, and right-hand swinging mode. The acceleration data exhibits different patterns across the axes under these various modes.

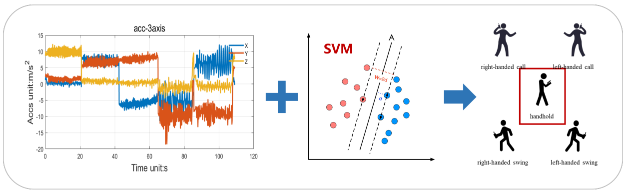

Figure 2. Estimation on carrying modes of mobile phone

Building on this, we selected the three-axis accelerometer values and their differences as features, combining them with our self-sampled dataset to train an SVM classifier using K-fold cross-validation. Subsequently, the trained classifier was employed to categorize user data, particularly focusing on those who remained in a handheld state throughout. We then estimated pedestrian trajectories based on the classified data. Using the step length formula and position estimation equations, we calculated the pedestrian trajectory as follows:

$$SL = 0.7 + 0.371(H - 1.75) + 0.227\frac{(SF - 1.79)H}{1.75} \quad (1)$$

$$N_{K+1} = N_K + SL_K \times \cos(\alpha_K) \quad (2)$$

$$E_{K+1} = E_K + SL_K \times \sin(\alpha_K) \quad (3)$$

where SF is the step frequency, H is the height, SL is the step length, α_K is the heading angle, (E_K, N_K) are the current position coordinates, and (E_{K+1}, N_{K+1}) are the coordinates of the next position.

https://doi.org/10.5194/isprs-annals-X-G-2025-1011-2025

2.3 Trajectory Clustering Based on 5G and WiFi

This paper combines the characteristics of numerous shops in the mall and rich WiFi information, utilizing the phenomenon of distance attenuation of WiFi signals. We employ the count of high-strength WiFi SSIDs as features for path clustering (Fig. 3).

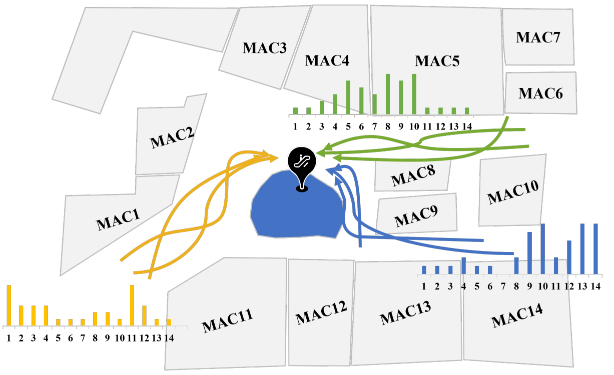

Figure 3. The occurrence frequency of received WiFi signals varies across trajectories from different directions

When multiple WiFi devices are installed in the same shop, variations in SSIDs can be achieved through capitalization or by adding suffixes. Thus, merging heterogeneous SSIDs of the same shop becomes a prerequisite for path clustering. After performing operations such as lowercasing and tokenization, we utilize the TF-IDF (Grootendorst, 2022) algorithm to convert SSIDs into vectors for clustering. The principle of the TF-IDF algorithm is as follows:

$$\text{TF-IDF}(w) = \text{TF}(d, w) \times \text{IDF}(w) \tag{4}$$

$$\text{IDF}(w) = \log\left(\frac{N}{N(w)}\right) \tag{5}$$

where $\text{TF}(d, w)$ represents the term frequency of word w in document d, and $\text{IDF}(w)$ denotes the inverse document frequency of word w, calculated as the logarithm of the ratio of total documents N to the number of documents containing word w ($N(w)$).

After vectorizing the text using TF-IDF, we apply the K-means clustering algorithm alongside the silhouette score for evaluation, selecting the best class for clustering. This allows for the merging of heterogeneous SSIDs from the same shop. Subsequently, we perform clustering analysis on the WiFi SSID counts using the same clustering and scoring algorithms to achieve path clustering for users transitioning between layers at the same landmark.

2.4 Trajectory Correction Based on Feature Extraction

After the aforementioned processing steps, we obtained trajectory clusters that converge at the same escalator point but originate from different directions. Since the multi-source data consists of transitions from outdoor to indoor environments, we used high-precision GNSS positioning results as the initial points for trajectory correction. The trajectories served as references for correcting trajectories within the same cluster. We employed a matching method based on feature point locations to achieve trajectory correction.

$$v_i = \frac{dist(P_i, P_{i-1})}{t_i - t_{i-1}} \tag{6}$$

$$a_i = \frac{v_i - v_{i-1}}{t_i - t_{i-1}} \tag{7}$$

$$\alpha_i = \left|\tan^{-1}\frac{y_{i+1} - y_i}{x_{i+1} - x_i} - \tan^{-1}\frac{y_i - y_{i-1}}{x_i - x_i - 1}\right| \tag{8}$$

$$\omega_i = \frac{\alpha_i}{t_i - t_{i-1}} \tag{9}$$

$$s_i = \frac{dist(P_{i-1}, P_i) + dist(P_i, P_{i+1})}{dist(P_{i-1}, P_{i+1})} \tag{10}$$

We denote the trajectory point P_i by (t_i, x_i, y_i), where t_i is the trajectory point timestamp information and (x_i, y_i) is the coordinate information. For each feature point, we choose a motion feature vector consisting of velocity v_i, acceleration a_i, steering angle α_i, steering angular velocity ω_i and curvature s_i for representation.

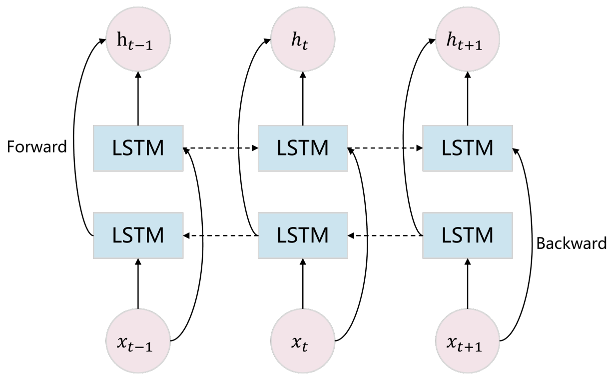

Figure 4. Bi-LSTM model

We design a Bi-LSTM model and use the time series data consisting of the feature vectors of this trajectory point and the trajectory points before and after it as inputs, and use the Bi-LSTM model to automatically extract the features of the sample data for classification training. Using the trained model, we extract the inflection points of the trajectory, combining the distance information between the inflection points and the landmark points, and initially screen the combinations of inflection points with high distance similarity. Then we extract the WiFi information at the inflection points, calculate the similarity of WiFi information between the inflection points, and obtain the most similar inflection point combinations between different trajectories. Finally, trajectory aggregation is achieved by inflection point aggregation.

2.5 Fingerprint Database Construction

Based on the corrected trajectories of the massive users, the database can be built by collecting the information on WiFi signal strength (e.g., RSSI), SSID, MAC addresses, and 5G base station information (e.g., base station ID and signal strength). In this step, the area of the interest is classified into grids with the area of 5 meter by 5 meter. Different trajectories within the same grid are associated as one control point (CP) and the measurements collected in one CP are merged in the database.

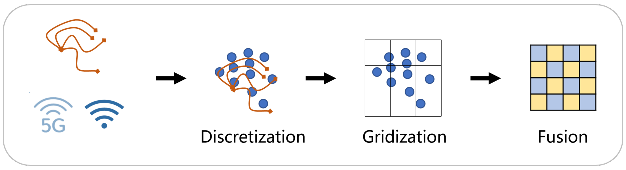

Figure 5. Generation of fingerprint database based on corrected trajectories

2.6 Estimation on the Location of POI

In order to build sematic map and assist positioning during the online estimation of the mobile users, we carry out the estimation on the POI. Based on the principle of the free-space propagation of the wireless signals, the distance between the user and the AP can be calculated according to the path loss model, i.e.,

$$L = 20lg(d) + 20lg(f) + K \tag{11}$$

where K is the environmental parameter. As is known, K is largely based on the specific surroundings, which is hardly known beforehand. Therefore, L can not be directly calculated. However, in most cases, for two locations in close distance, it is reasonable to assume that, the propagation environments are similar and the environmental parameter is equal. Thus, the difference in received signal strength $\Delta L_{i,j}$ is logarithmically related to the ratio of distances d_i/d_j and the k can be eliminated.

$$\Delta L_{i,j} = L_i - L_j = 20 \lg \frac{d_j}{d_i}. \tag{12}$$

We assume that (x_i, y_i) and (x_j, y_j) are the positions of the users and (x, y) are the location of the AP. By further mathematical operation, we can get

$$(x - \frac{p^2 \times x_j - x_i}{p^2 - 1})^2 + (y - \frac{p^2 \times y_j - y_i}{p^2 - 1})^2 = \frac{p}{p^2 - 1}^2 \times l^2 \tag{13}$$

where $p = 10^{\frac{RSS_j - RSS_i}{20}}$ and $l = \sqrt{(x_i - x_j)^2 + (y_i - y_j)^2}$. The (13) is valid when $RSS_j - RSS_i \neq 0$, while in the case that $RSS_j - RSS_i = 0$, we can get

$$(x_j - x_i)x - (y_i - y_j)y + \frac{y_i^2 - y_j^2}{2} + \frac{x_i^2 - x_j^2}{2} = 0 \tag{14}$$

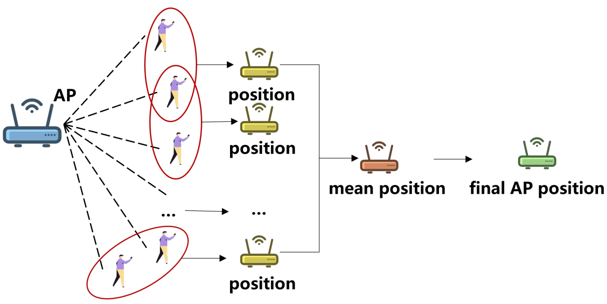

Figure 6. WiFi AP position estimation based on iteration

Based on the above, the location of the POI can be derived. By averaging, we can get the final position of POIs. The scheme is described in Fig. 6

2.7 Online Positioning with Fingerprint Database

We carry out two steps for on-line positioning. In the first step, POI-based coarse localization is applied. By comparing the received WiFi signals from a specific AP with POIs in the database, the location of the mobile can be coarsely estimated near the POI. On the basis of coarse localization, a random forest algorithm is applied for precise localization, by utilizing the WiFi and 5G fingerprint databases. The real-time collected WiFi and 5G signal features serve as input to a random forest model, which is pre-trained by labels and the signals of WiFi and 5G in the fingerprint databases. The two-step matching method not only allows for rapid estimation of the device's location by reducing the search space, but also improves the efficiency of precise localization.

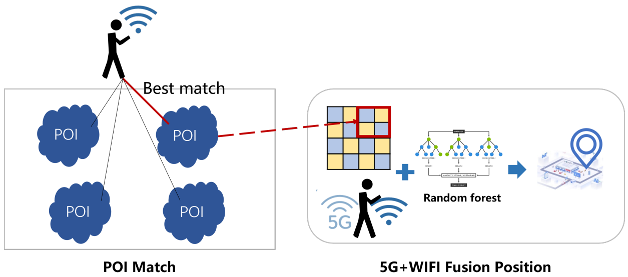

Figure 7. POI-based coarse localization and fusion fine localization

3. Experiments and Discussion

3.1 Experimental Settings

The experiment was conducted on the first floor of Wuhan Intime Shopping Mall, covering an area of approximately 67 × 138 m², as shown in Fig. 8. There are 5 escalators on this floor, and we designated the escalator locations as landmark points. The experimental data were collected by the mall staff using their personal Android smartphones, and the experimental routes followed paths from outdoor areas to each landmark point. The types of data collected include inertial navigation data, WiFi data, and 5G NR data. The inertial navigation data was recorded at a frequency of 100 Hz, while the 5G NR and WiFi data were collected at a frequency of 0.2 Hz. A total of 185 sets of data were collected.

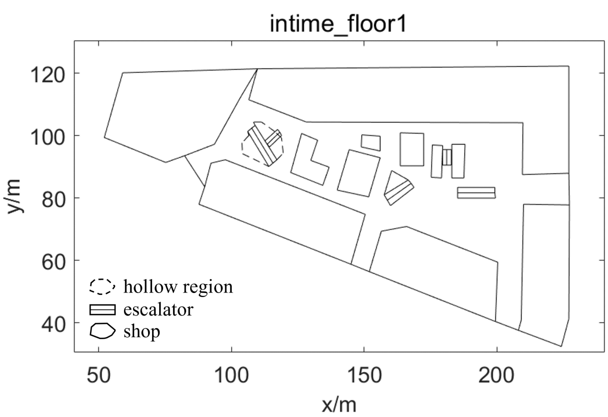

Figure 8. Experimental area

3.2 Results of Crowdsourced Data Processing

We use mobile phones to collect three-axis acceleration data samples under five walking states: hand-held, left-handed phone call, right-handed phone call, left-handed arm swing, and right-handed arm swing, with a sample size of 231. The values and differences of the acceleration are extracted as features, and the SVM classification model is trained using the K (K=10) folded cross-validation method to divide the training set and the test set.

Walking pattern is performed on the user data using the trained model and some of the results are shown in Fig. 9, where 1 is handheld, 2 is left-handed phone call, 3 is right-handed phone call, 4 is left-handed arm swing and 5 is right-handed arm swing. The result of the third figure indicates that the user's mobile phone stays in handheld posture throughout the walking, i.e., the user data is valid.

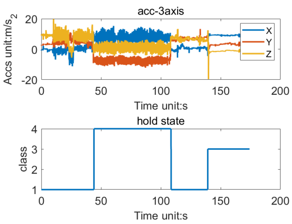

(a)

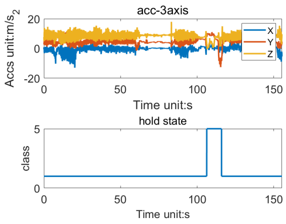

(b)

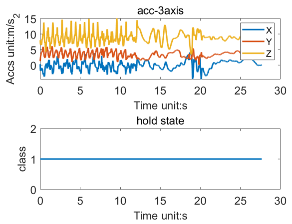

(c)

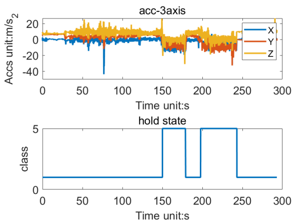

(d)

Figure 9. Mobile posture determination: during walking, there are posture changes in (a), (b), and (d), while (c) maintains a handheld posture throughout.

Based on the content of Section 2.2, we can obtain the trajectory of users who held their devices continuously, as shown in Fig. 10(a). After obtaining the trajectories, based on the content of Section 2.3, we got the results of clustering of the users with different incoming directions from the same landmarks. The accuracy of clustering algorithm at different landmarks is 93.33%, 84.62%, 84.62%, 83.33%, and 100% respectively. The clustering accuracy is high and the clustering algorithm is able to perform the dataset clustering classification well in most of the cases.

After the classification is completed, in order to correct the trajectories, we analyse the GNSS data received at the entry point. We find trajectories with more reliable GNSS accuracy at the entry point among 59 trajectories and correct the trajectories by the position of the entry point as the reference trajectories for the subsequent corrections. After obtaining the reference trajectory, we perform trajectory correction based on inflection point features for the remaining uncorrected trajectories of the same class as the reference trajectory.

We choose Bi-LSTM model to implement the inflection point extraction. For this purpose, we collected a total of 2138 trajectory points as a dataset, and performed feature extraction and labelling on the original dataset. Then, we divided the training set and test set in a ratio of 7:3, divided the training set into batches, and performed iterative training and optimised the model parameters in batches. The accuracy of the model on the test set is 93.1%, and finally, we use the trained Bi-LSTM model to judge the inflection point of the obtained trajectory data. Then the similarity between the inflection points on the uncorrected trajectory and the reference trajectory is calculated separately by combining the two metrics of distance and WiFi similarity, and the trajectory aggregation correction is achieved based on the inflection point with the highest similarity.

Ultimately, we obtained all available trajectories (Fig. 10(b)) and constructed a positioning fingerprint database (Fig. 10(c)). From the results, the obtained corrective paths cover most of the ground floor of the mall, and the constructed fingerprint database can support the navigation and localisation of pedestrians. However, there are still cases of missing fingerprint database in some areas.

3.3 Online Positioning

3.3.1 Static Data Testing: In order to verify the validity of the acquired trajectories and the constructed fingerprint database, we selected 10 test points within the experimental area, distributed as shown in Fig. 11. A Huawei P40 mobile phone was used to collect WiFi and 5G NR data at the corresponding stationary locations, with an acquisition duration of 5 minutes and a sampling frequency of 1Hz.

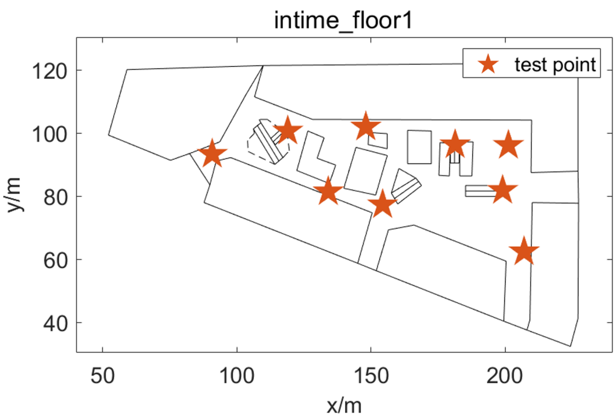

Figure 11. The Distribution of test points

When WiFi data is involved in localization, we add a fingerprint point screening process before each test data is localized. The MAC addresses of the five APs with the highest signal strength in the test data are used as a reference. Only the fingerprint points where the MAC addresses of the top five APs overlap with this reference are retained for the localization process. For comparison, in terms of localization sources, we consider WiFi and the combination of WiFi and 5G NR. The results are shown in Fig. 12.

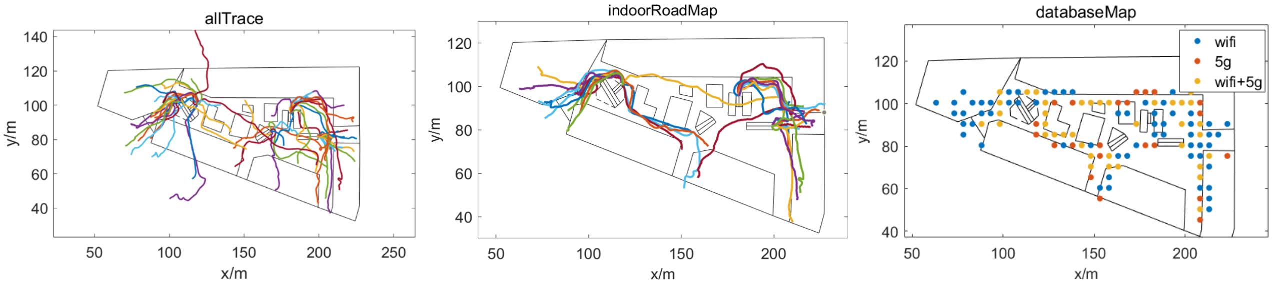

(a) (b) (c)

Figure 10. Fingerprint database construction. (a) uncorrected trajectories; (b) corrected trajectories; (c) WiFi and 5G NR fingerprint database.

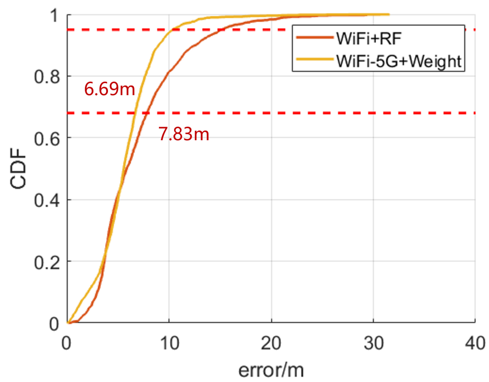

Figure 12. Positioning errors in static testing

When the signal source is WiFi, the mean positioning error using the random forest algorithm is 6.95 meters, with a standard deviation of 4.26 meters. Overall, the WiFi-based positioning performs well and meets the accuracy requirements for user navigation in shopping malls. However, in some cases, the positioning error exceeds 10 meters, indicating insufficient stability. This instability is attributed to a two-month gap between the test and fingerprint data, during which significant changes occurred around two test points, affecting nearby shop information and leading to higher errors. When both WiFi and 5G NR are used as signal sources, the wide-area accuracy of WiFi and the local precision of 5G NR complement each other for enhanced localization. The mean positioning error is reduced to 5.75 meters, with a standard deviation of 2.99 meters. This represents a 17% improvement in accuracy compared to WiFi localization alone. In conclusion, the crowdsourcing-based solution for WiFi and 5G signal map construction and localization proposed in this paper can achieve high-precision, high-reliability positioning in consumer-grade scenarios while maintaining a low-cost indoor localization system.

3.3.2 Dynamic Data Testing: To validate the accuracy of the acquired trajectories and the constructed fingerprint database, we selected both static test points and three dynamic routes within the experimental area. The lengths of the routes were 187.40 meters, 148.25 meters, and 260.84 meters, respectively. Signal data was collected at a frequency of 0.2 Hz, while inertial navigation data was recorded at 100 Hz using a Huawei P40 smartphone. Simultaneously, high-precision inertial navigation equipment (MTi-680G) was used for synchronized data collection. With the aid of landmark points, trajectory reproduction was achieved, providing the reference trajectory for experimental comparison.

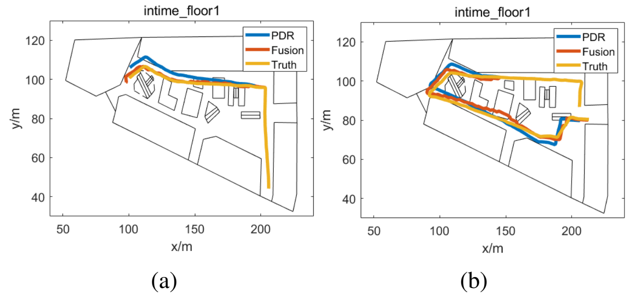

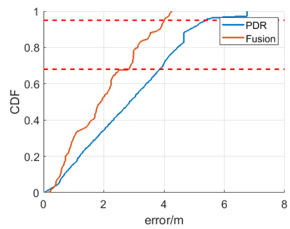

(c)

Figure 13. Dynamic positioning results and errors. (a) positioning results for trajectory 1; (b) positioning results for trajectory 2; (c) dynamic positioning errors.

From the static test results, we know that the average positioning accuracy of the fingerprint database is 5.75 meters. This accuracy is sufficient for mall-level navigation, meaning it can effectively guide users along the path. However, achieving highly accurate dynamic positioning using only the WiFi + 5G NR database constructed in this study remains challenging. Therefore, in dynamic testing, we evaluate the usability of the fingerprint database by assessing the extent to which fingerprint localization results correct the PDR results.

From the perspective of positioning accuracy, fusion localization demonstrates a significant improvement compared to PDR alone. The average positioning error is reduced by approximately 30%, and the 2-σ positioning error is improved by more than 22%. The integration of fingerprint localization effectively suppresses the error drift of PDR, further validating the effectiveness of the crowdsourcing-based solution for WiFi and 5G signal map construction and positioning proposed in this paper.

shop name	HUAWEI	SUNION	Chow_tai_fook	Goldstyle	innisfree	intime365	laoFengXiang
error/m	1.34	2.96	0.03	9.49	1.44	4.42	9.61
shop name	maancoffee	mac	sephora	stacatto	urshop	voyah	juduo
error/m	2.27	4.24	2.77	8.31	8.13	3.17	3.16

Table 1. Errors in shop location positioning

3.4 Semantic Map Acquisition

Previously we obtained some WiFi AP locations on the ground floor of the Yintai shopping mall through some known track points. We can combine the WiFi AP locations with the ssid information to obtain the approximate locations of the merchants on the ground floor of the mall. Therefore, we use all the acquired trajectory data to project the shop locations on the ground floor of the mall to construct a semantic map.

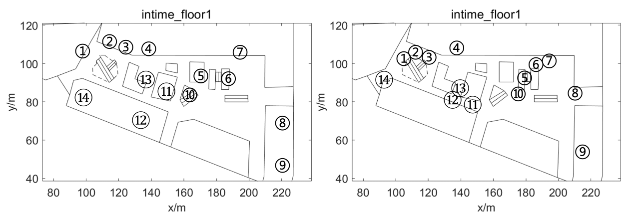

(a) (b)

Figure 14. Semantic map construction: (a) correct semantic map; (b) computed semantic map.

We compare the projected location with the real value, and the error of each location is shown in Table 1. The mean value of the positioning error is 4.38 m, and the standard deviation is 3.18 m. Combining these two indicators, we can conclude that the results of the shop position projection are highly accurate. However, because we ignore the existence of height difference in the calculation process, the projected position error is larger for some devices with higher hanging height, such as stacatto. There is also a special case where the brand urban revivo has shops on both the first and first floors of the mall, and it is impossible to tell where the APs in our data originate from, which is also not analysed in this paper. In the future, we will analyse in the direction of AP signal strength and AP signal strength change to determine the AP source. Overall, we can obtain a high quality semantic map without using the map. When the user walks into the shopping mall, combining the positioning and semantic map, the phone can automatically recommend services related to the nearby shops, which realises the combination of positioning and life services.

4. Conclusion

To address the challenges of constructing a fingerprint database in the absence of indoor maps and uncalibrated magnetometers, this paper proposes a novel method for fingerprint database acquisition based on sparse features. This method encompasses three components: trajectory reproduction under multiple postures, feature-based trajectory aggregation correction, and point of interest (POI) location acquisition. In trajectory correction, we introduce the concept of clustering, using a reference trajectory that has been corrected via a specific method to correct all trajectories within the same cluster. For trajectory clustering, we utilize the WiFi SSID count instead of trajectory shape as a feature, which resolves the issue of varying trajectory shapes in open environments. Additionally, we propose a method for POI location acquisition to facilitate the construction of semantic maps alongside localization services.

We selected the first floor of a large shopping mall as the experimental site to validate the proposed method’s performance. The experimental dataset consists of 185 user-collected trajectories. The accuracy of trajectory clustering exceeds 80%, with an average positioning error of 5.73 meters for stationary test points and an average error of 4.38 meters for POI location estimations. These results validate the feasibility and effectiveness of the proposed methods, as well as the stability of the trajectory clustering approach and the accuracy of the corner point detection algorithm.

It is important to note that the proposed method relies on sparse features to obtain trajectory endpoint information. Therefore, further research is needed on how to acquire trajectory endpoint information, including the partitioning of multi-floor behaviors under unstable barometric conditions, the determination of user groups arriving at the same landmark, and the precise acquisition of initial heading direction.

Acknowledgment

This work is supported by the National Natural Science Foundation of China (Grant No. 42171417), Jiangsu Province Science and Technology Major Special Project: Research and Development of Key Technologies for 6G Ubiquitous High-Precision Positioning (Grant No. BG2024003) and Guangxi Science and Technology Major Project (Grant No. AA22068072).

References

Bellavista-Parent, V., Torres-Sospedra, J., Perez-Navarro, A., 2021. New trends in indoor positioning based on wifi and machine learning: A systematic review. *2021 International Conference on Indoor Positioning and Indoor Navigation (IPIN)*, IEEE, 1–8.

Grootendorst, M., 2022. BERTopic: Neural topic modeling with a class-based TF-IDF procedure. *arXiv preprint arXiv:2203.05794*.

Groves, P. D., 2015. Principles of GNSS, inertial, and multisensor integrated navigation systems, [Book review]. *IEEE Aerospace and Electronic Systems Magazine*, 30(2), 26–27.

Hu, Y., Qian, F., Yin, Z., Li, Z., Ji, Z., Han, Y., Xu, Q., Jiang, W., 2022. Experience: practical indoor localization for malls. *Proceedings of the 28th Annual International Conference on Mobile Computing And Networking*, MobiCom ’22, Association for Computing Machinery, New York, NY, USA, 82–93.

Jang, B., Kim, H., 2018. Indoor positioning technologies without offline fingerprinting map: A survey. *IEEE Communications Surveys & Tutorials*, 21(1), 508–525.

Junoh, S. A., Pyun, J.-Y., 2023. Enhancing indoor localization with semi-crowdsourced fingerprinting and gan-based data augmentation. *IEEE Internet of Things Journal*.

Lan, T., Wang, X., Chen, Z., Zhu, J., Zhang, S., 2022. Fingerprint augment based on super-resolution for WiFi fingerprint based indoor localization. *IEEE Sensors Journal*, 22(12), 12152–12162.

Liu, W., Zhang, Y., Deng, Z., Zhou, H., 2023. Low-cost indoor wireless fingerprint location database construction methods: A review. *IEEE Access*, 11, 37535–37545.

Ruan, Y., Chen, L., Zhou, X., Guo, G., Chen, R., 2022. Hi-Loc: Hybrid indoor localization via enhanced 5G NR CSI. *IEEE Transactions on Instrumentation and Measurement*, 71, 1–15.

Ruan, Y., Chen, L., Zhou, X., Liu, Z., Liu, X., Guo, G., Chen, R., 2023. iPos-5G: Indoor Positioning via Commercial 5G NR CSI. *IEEE Internet of Things Journal*, 10(10), 8718-8733.

Ruizhi, C., Liang, C., 2017. Indoor Positioning with Smartphones: The State-of-the-art and the Challenges. *Acta Geodaetica et Cartographica Sinica*, 46(10), 1316.

Sun, M., Wang, Y., Xu, S., Yang, H., Zhang, K., 2021. Indoor geomagnetic positioning using the enhanced genetic algorithm-based extreme learning machine. *IEEE Transactions on Instrumentation and Measurement*, 70, 1–11.

Wang, Y., Kuang, J., Liu, T., Niu, X., Liu, J., 2023. CrowdMagMap: Crowdsourcing based magnetic map construction for shopping mall. *IEEE Internet of Things Journal*.

Yang, H., Chen, L., Liu, H., Zhu, G., 2024. Dynamic Feature-fused Localization with Smartphones Exploiting 5G NR SSB and Wi-Fi for Indoor Environments. *IEEE Transactions on Instrumentation and Measurement*.

Zhao, Y., Zhang, Z., Feng, T., Wong, W.-C., Garg, H. K., 2020. GraphIPS: Calibration-free and map-free indoor positioning using smartphone crowdsourced data. *IEEE Internet of Things Journal*, 8(1), 393–406.